# SURFACE SUBSIDENCE MONITORING IN GANZHOU AREA BASED ON SBAS-INSAR

Xinyi Li [1], Lv Zhou [1, 4*], Jun Ma [2], Zilin Zhu [3], Xin Li [4, 5], Ling Huang [1]

[1] College of Geomatics and Geoinformation, Guilin University of Technology, Guilin 541004, China - (Lixinyi_sherry@163.com, zhoulv@glut.edu.cn, huangling_whu@126.com)
[2] China Railway Siyuan Survey And Design Group Co., LTD, Wuhan 430063, China - (yangzhiqou.student@sina.com)
[3] BeiJing Vastitude Technology Co., Ltd, Beijing 100191, China - (zlzhu@vastitude.cn)
[4] Guangxi Key Laboratory of Spatial Information and Geomatics, Guilin University of Technology, Guilin 541004, China - (lixin2017@chd.edu.cn)
[5] College of Geology Engineering and Geomantic, Chang'an University, Xi'an 710054, China

**KEY WORDS:** SBASInSAR, surface subsidence , time series analysis,  Ganzhou, temporal-spatial characteristics

**ABSTRACT:**

In this paper, we first obtained the temporal-spatial changes of surface subsidence in Ganzhou area based on SBAS-InSAR technology using 24 scenes Sentine-1A images covering the Ganzhou area from 2018 to 2020. Then we studied the surface subsidence characteristics in the study area. Finally, the relationship between surface subsidence and factors such as precipitation, human engineering activities, groundwater extraction, and sediment accumulation were analyzed in Ganzhou area. The results showed that : 80% of the sedimentation rate was -5.4~3.0 mm/a in the study area; serious subsidence areas were mainly located in Ganxian District, which annual average subsidence rate reached -26.4mm/a, and the time series of surface subsidence was accompanied by certain seasonal changes; the seasonal changes in surface subsidence were related to rainfall and groundwater extraction, in addition, the surface subsidence was obviously affected by human engineering activities and river sediment accumulation.

## 1. INTRODUCTION

With the progress of urbanization in various regions, the urban surface subsidence phenomenon has become more and more common, and it has a serious impact on the sustainable development of social economy (Wu et al., 2019). As the largest city in Jiangxi Province, geological disaster frequently occurs in Ganzhou. At the same time, the increase in population and the rapid progress of urbanization have aggravated the surface subsidence of Ganzhou. In order to prevent geological disasters and environmental damage, monitoring the surface subsidence of Ganzhou City has important significance and practical value. At present, traditional surface subsidence monitoring mainly includes groundwater dynamic monitoring, conventional precision levelling, layer mark monitoring, and global navigation satellite system. Although the above methods can obtain high-precision monitoring results, they are costly and need to enter the study area for observation. It is difficult to obtain large-scale, high-spatial resolution monitoring information of surface subsidence effectively (Chen et al., 2020). As an effective technology for monitoring ground deformation, differential interferometric synthetic aperture radar (D-InSAR) can obtain surface deformation information within a short time which have spatial continuity, and the monitoring accuracy is high. It can effectively overcome the shortcomings of the above-mentioned traditional monitoring methods such as low spatial resolution and high cost. This technology has gradually been applied to related fields such as landslide monitoring, glacier movement and earthquake deformation (Singleton et al., 2014; Sánchez-Gámez et al., 2017; Hu et al., 2012). However, because the DInSAR technology is susceptible to the limitation of temporal and spatial decorrelation and effect of atmospheric insulation in the process of monitoring the surface subsidence and deformation, which leads to the low accuracy and reliability

of the obtained monitoring results (Chen et al., 2020). Therefore, in order to reduce the influence of temporal and spatial decorrelation and atmospheric delay effectively, the small baseline subset interferometric synthetic aperture radar (SBAS-InSAR) technology is proposed which is based on traditional D-InSAR technology. This method combined SAR images into several subsets, and used the least squares method to solve the deformation sequence of the subset, and use the singular value decomposition method to solve multiple small baseline sets jointly, then obtain the deformation sequence of the entire time span, which further improves the accuracy of surface subsidence monitoring (Berardino et al., 2002). The SBAS-InSAR technology was used to study the surface deformation of South Wales, and the study results analysed the causes of surface deformation in the coalfields area (Luke et al., 2015); Zhou et al. (2016) summarize the development law and spatial distribution characteristics of surface subsidence in Wuhan city based on SBAS-InSAR technology using Sentinel-1A image data; in order to elucidate and monitor the nature of the spatial extent during and after the flood event in the Lorestan Province, Iran, and to evaluate flood-induced ground displacement, Ali (2021) used the time series Sentinel-1 images and SBAS-InSAR technology.

Although SBAS-InSAR technology has been widely used in urban surface subsidence monitoring research, there is a few researches on Ganzhou urban area using the small baseline subset interferometric method. This paper used SBAS-InSAR technology to monitor and analyse urban surface subsidence in Ganzhou, Jiangxin based on the Sentine-1A images. Then the temporal and spatial distribution of surface subsidence in the study area from 2018 to 2020 can be obtained. This paper subsequently verified the reliability and accuracy of the SBAS-InSAR technology in monitoring urban surface subsidence.

---

\* Corresponding author

Finally, human rainfall and engineering activities, other factors were combined to discuss and analyze the characteristics of surface subsidence in the study area.

## 2. METHODOLOGY

The SBAS-InSAR technology can overcome the spatial and temporal decorrelation phenomenon for several small subsets based on spatial and temporal baseline threshold combination time series. Firstly, the interference pair sets were obtained based on spatial and temporal baseline thresholds; then the phase information in the collection was reached by the least squares method; subsequently, the minimum cost flow (MCF) method can be used to perform phase unwrapping and using the surface subsidence result of a single differential interference as the observation; finally, the surface subsidence sequence was derived by using least squares algorithm or singular value decomposition (SVD) method (Mo et al.,2020), the main steps are as follows (Hooper et al., 2007):

(1) Within the image acquisition time ($t_0$, $t_1$,..., $t_n$), one scene among the N+1 scenes Sentinel-1A images in the study area was selected to be the super master image and registered all auxiliary images to it. After combining interference baselines and appropriate time, the N+1 images can generate M differential interference graphs, and M meets the following conditions:

$$\frac{N+1}{2} \le M \le \frac{N(N+1)}{2} \tag{1}$$

(2) Assuming the interferogram j ∈ (1,2,...,M) were generated by combining SAR acquisitions at $t_A$ and $t_B$ ($t_B > t_A$), so the interference phase of a pixel with the azimuth coordinate $x$ and the distance coordinate $r$ can be expressed as:

$$\delta\varphi_{j,def} \approx \frac{4\pi}{\lambda}[\mathrm{d}(t_B,x,r) - \mathrm{d}(t_A,x,r)] \tag{2}$$

After ignoring the phase of atmospheric delay, residual terrain, and noise, the interferometric phase expression can be simplified to:

$$\delta\varphi_j = \varphi_B(x,r) - \varphi_A(x,r)$$
$$\approx \frac{4\pi}{\lambda}[\mathrm{d}(t_B,x,r) - \mathrm{d}(t_A,x,r)] \tag{3}$$

Where $\varphi$ is the interference phase; $\lambda$ is the wavelength of the radar signal; $\varphi_A(x,r)$ and $\varphi_B(x,r)$ are the SAR image phase values at $t_A$ and $t_B$; $\mathrm{d}(t_A,x,r)$ and $\mathrm{d}(t_B,x,r)$ are the cumulative subsidence in the direction of sight at $t_A$ and $t_B$ relative to $\mathrm{d}(t_0,x,r)=0$.

(3) According to formula (3), the interference phase value can be expressed by the product of the difference between the two acquisition times and the average rate $v_j$ in this time period, which is:

$$v_j = \frac{\varphi_j - \varphi_{j-1}}{t_j - t_{j-1}} \tag{4}$$

Therefore, the phase value of the $j$-th number scene interference graph can be expressed as:

$$\sum_{k=t_{A,j}}^{t_{B,j}} (t_k - t_{k-1})v_k = \delta\varphi_j \mathrm{j} \tag{5}$$

Which is, the rate integration of each period in the time interval of the main image and the auxiliary image, rewritten into a matrix form as follows:

$$\mathbf{B}v = \delta\varphi \tag{6}$$

Among them, $\mathbf{B}$ is the coefficient matrix of $\mathbf{M} \times \mathbf{N}$.

The least square method can be used to solve the subsidence rate $v$ when the coefficient matrix $\mathbf{B}$ is full rank, and if the matrix $\mathbf{B}$ is singular, the singular value decomposition (SVD) method can be used to obtain the minimum norm solution of the subsidence rate, which can reach the subsidence in the corresponding time interval based on the time interval of the SAR images.

## 3. MONITORED OBJECT AND MEASUREMENT CAMPAIGN

### 3.1 Study Area

Ganzhou City (113°54′E~116°38′E, 24.°29′N~27°09′N) is the most populous and largest city in Jiangxi Province, located in the upper reaches of Ganjiang River and southwestern Jiangxi. Ganzhou City is also the most important grain, oil, forest and fruit production area in Jiangxi Province. However, the plant destruction and soil erosion are getting worse because of long-term unreasonable economic activities, so the ecological environment is a urgent problem need to improve (Hong et al., 2016). In addition, heavy rainfall and heavy rain during the flood season often trigger mountain torrents in Ganzhou, and it caused frequent occurrence of sudden geological disasters such as avalanches, landslides, and ground subsidence. The central part of Zhanggong District is the urban area with the confluence of Zhangjiang River and Gongjiang River in its territory, and it's rich in water resources (Liu et al., 2020). Ganxian District is connected to the west of Zhanggong District, which is located in the upper reaches of Ganjiang River, and it's also a part of Ganzhou's downtown area. This paper selected the downtown area of Ganzhou (a part of Ganxian District and a part of Zhanggong District) as the study area. The clipping range is shown in Figure 1, and the coverage is about 500km².
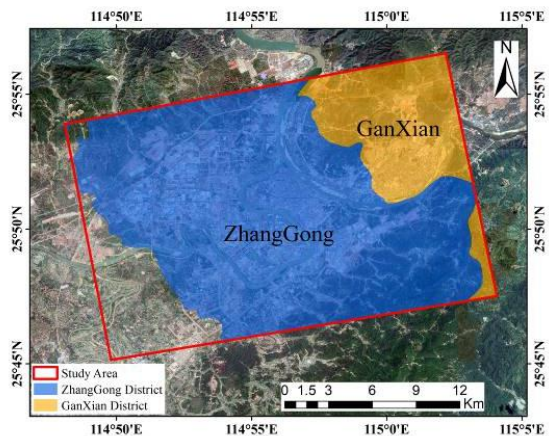


**Figure 1.** Geographical scope of the study area

### 3.2 Data source introduction

This paper selected 24 scenes Sentinel-1A SAR images in descending orbit mode covering Ganzhou area from September 2018 to August 2020. The basic satellite parameters are shown in Table 1, which provided by the European Space Agency (ESA). The precision orbit data was the satellite precision orbit POD (precise orbit ephemerides) provided by the European Space Agency. In addition, the DEM data used in the data processing process comes from the SRTM V4 DEM with a resolution of 90m which provided by the National Aeronautics and Space Administration of the United States (NASA).

| Satellite model | Sentinel-1A |
|---|---|
| Orbit direction | Descending orbit |
| Angle of incidence | 39.1° |
| Band | C |
| Polarization mode | VV |
| Amount | 24 |
| Time span | 2018-09-10~2020-08-18 |

**Table 1.** Basic parameters of satellite data

## 4. DATA PROCESSING

Using Sentinel-1A satellite images and the data processing software called SARscape to monitor the surface subsidence of the study area, the data processing flow is shown in Figure 2. The main processes are as follows. Firstly, importing the required downloaded data into SARscape, and clipping the original images to obtain the temporal SLC data of the study area. Then selected the image on July 19, 2019 as a super master image, and all the remaining images were registered with it, 203 pairs of differential interference graphs were generated, the interference graph of the Temporal and spatial baseline distribution can be shown in Figure 3, where the yellow dot represented the super master image. Subsequently, all paired interferences were performed interference processing, which including coherence generation, interferogram flattening and filtering, phase unwrapping, and calculation of coherence coefficients, and the results showed that most of the study area had good interference, and there were no extremely undesirable interference pairs in the generated data, so all data pairs can be retained. In addition, 20-30 ground control points (GCP) were selected in the flat and stable area, the GCPs were able to re-level all the data, and then the slope phase was estimated by using the cubic orbital refinement polynomial in the phase unwrapping result. Finally, the surface subsidence rate of final each time period can be derived by using the least square method to solve the phase unwrapping result.
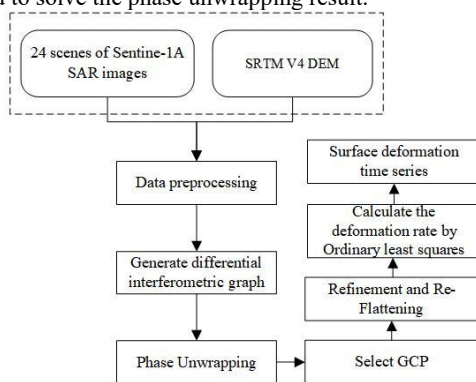


**Figure 2.** Data processing flow
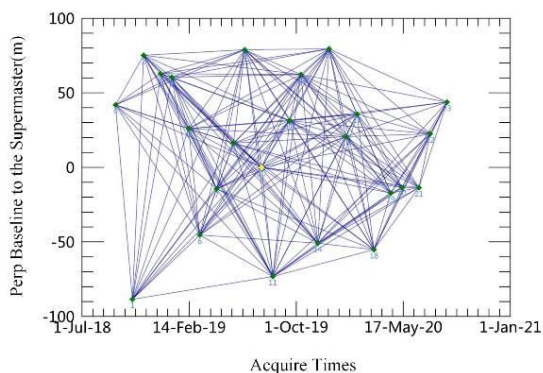


**Figure 3.** Temporal and spatial baseline distribution of the interference graph

## 5. RESULT ANALYSIS

### 5.1 Analysis of the overall situation of surface subsidence in the study area

Figure 4 showed the surface subsidence rate of the study area from September 2018 to August 2020. The surface subsidence rate of the entire study area ranged from -26.4 to 19.8 mm/a, and the area with a surface subsidence rate was between -5.4 and 3.0 mm/a accounted for more than 80% of the entire study area. The surface subsidence degree was relatively slight, which can be regarded as basically stable. The overall surface subsidence rate of Ganxian District in the study area was larger than that of Zhanggong District, and the surface subsidence rate of Zhanggong area was smaller and relatively stable, as shown in Figure 5. In terms of township boundaries, the surface deformation in Chutan Town, Meilin Town, Shuidong Town and Shahe Town were relatively serious. As a result, the research was focused on several areas with serious continuous surface subsidence.
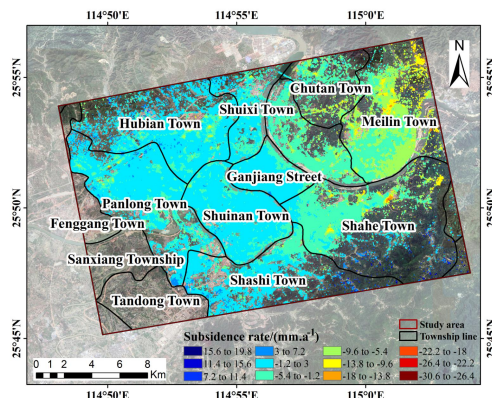


**Figure 4.** Surface subsidence rate in the study area from September 2018 to September 2020
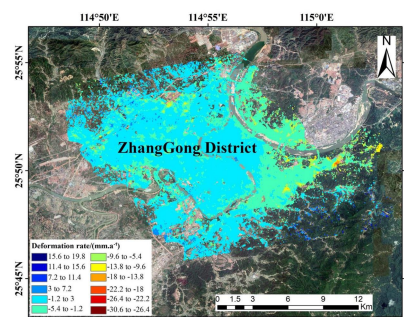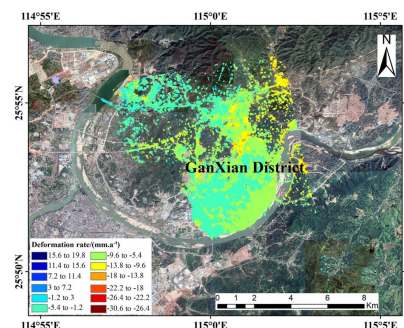


**Figure 5.** Comparison between surface subsidence profiles of Zhanggong District and Ganxian District

In order to explore the causes and influencing factors of the above-mentioned continuous and serious surface subsidence, this paper selected 7 study points in the study area to facilitate the follow-up study, as shown in Figure 4. Figure 6 showed the cumulative surface subsidence of the seven study points during the study period. Among them, P5 and P6 were stable points, and P1, P2, P3, P4, and P7 are the points selected in each obvious surface subsidence area. The cumulative surface subsidence of the stable study points fluctuate slightly between -4.2 and 1.7mm/a, and the study points P1, P2, P3, P4, and P7 have substantial surface subsidence relative to the two stable points. The following will discuss and further analyse the precipitation, human engineering activities, groundwater extraction, and sediment accumulation by combining Ganzhou's terrain, climate and overall situation.
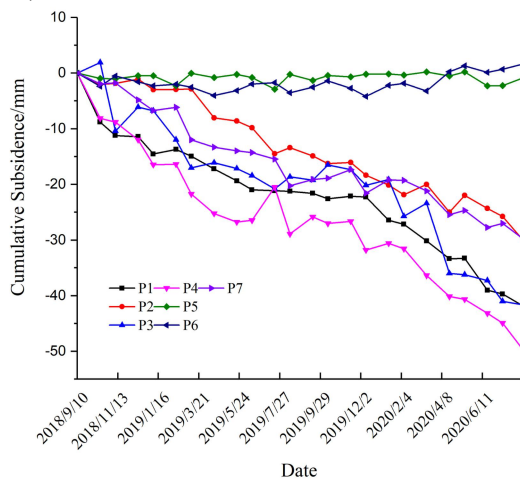


**Figure 6.** Cumulative surface subsidence of each study point

.
**5.2 Accuracy assessment**

After working out the statistical analysis of the standard deviation's sedimentation rate in the study area, it can be seen that the standard deviation of the monitoring points' average rate in the study area was 0.05 to 5.96 mm/a, and the probability density function graph shown in Figure7. Among them, monitoring points with a rate standard deviation below 3mm/a accounted for 99.32% of all.
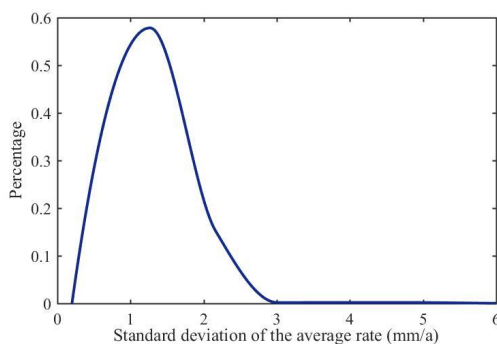


**Figure 7.** The probability density function of the standard deviation of the average rate

**5.3 The relationship between rainfall and surface subsidence in Ganzhou area**

Figure 8 shows that the cumulative surface subsidence from March to July of P1, P2, P3, P4, and P7 was larger than that in the other months each year. Moreover, Ganzhou has a subtropical monsoon climate, the rainy season is from March to

June, and the flood season is from April to June. During the flood season, the rainfall intensity is high and heavy rainstorms often trigger mountain torrents, which in turn causes sudden geological disasters such as the river's water level soaring, sudden collapses, landslides, and surface subsidence (Peng et al., 2017). In order to study the correlation between rainfall and surface subsidence in the study area, this paper selected the monthly average rainfall data of the NO.57993 meteorological station in Ganzhou and the cumulative surface subsidence of five study points which include P1, P2, P3, P4 and P7 during the study period for comparison and analysis, the result can be shown in Figure 8 below, from which showed the five study points varied seasonally. To fully consider the impact of rainfall on the surface subsidence in the study area, grey correlation analysis can be used to quantitative analysis. The correlation results were obtained with the rainfall to be the influencing factor, which can be shown in Table 2 below. The correlations between the subsidence variation and rainfall of the above five study points were about 0.6, which showed that there was a certain relationship between the variation of surface subsidence rate and rainfall in the study area.
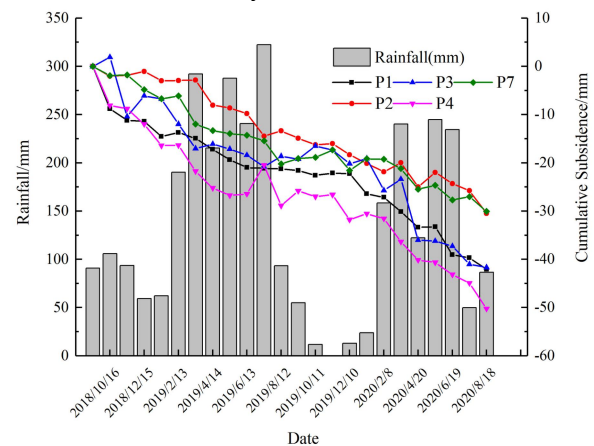


**Figure 8.** Comparison of rainfall and surface subsidence rate

| Study point | P1 | P2 | P3 | P4 | P5 | P6 | P7 |
|---|---|---|---|---|---|---|---|
| Correlation | 0.57 | 0.59 | 0.58 | 0.56 | 0.62 | 0.61 | 0.58 |

**Table 2.** Correlations between cumulative surface subsidence of study points and rainfall

**5.4 The relationship between human engineering activities and surface subsidence in the study area**

Human engineering activities include building construction, road construction, etc. In the case of incomplete protective measures, long-term and excessive human engineering activities will accelerate the subsidence of surface and may cause other geological disasters. Zhanggong District is the old city of Ganzhou City, while Ganxian District is a new city. Therefore, Ganxian has a large number of human projects under construction, and the density of underground soil was relatively looser than that of Zhanggong District. In addition, the overall surface subsidence of Ganxian District is more serious than in Zhanggong District because of the urban planning and construction, as shown in Figure 5. According to the comparison of the figure, it can be seen that the distribution area of     buildings and public roads has high consistency with the surface subsidence area. The investigation showed that there were signs of human engineering activities around the study points include P1, P2, and P7, as shown in Figure 9. P1 was located at an intersection of Gaoxin highway and Chengbei

highway in Meilin Town, and P7 was located in Fuyutang Village, Shahe Town, adjacent to a highway under construction. The project of Gaoxin highway was completed at the end of 2018, and the project of Chengbei highway was completed at the end of 2019. The maximum accumulative surface subsidence at P1 reached 42.1mm, and P7 reached 30.1mm. Ganzhou's highway mileage was relatively large, and highway construction continued to develop (Peng et al., 2017), so it was speculated that serious surface subsidence of P1 and P7 were related to road construction. P2 was located near the residential area under construction (Xinlidongyuan neighbourhood in the Meilin Town), and the maximum accumulative surface subsidence reaches 30.5mm. It can be seen that construction has a great impact on the Xinlidongyuan neighbourhood area. In summary, the human engineering activities had a strong correlation with the surface subsidence of the study area.
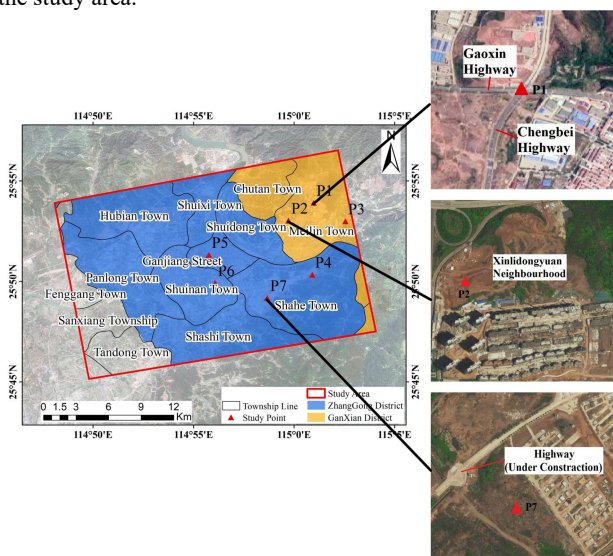


**Figure 9.** Satellite images around P1, P2, and P7 and the place of study points

## 5.5 Groundwater extraction

With the development of China's economy and technology and the increase of population, the demand for water resources in China is increasing day by day, which has led to an increasing amount of groundwater extraction (Lv et al., 2020), and triggered a series of geological disasters. In 2018, the amount of groundwater resources in Ganzhou reached 6.892 billion cubic meters. At the same time, the amount of groundwater consumption reached 169 million cubic meters, accounting for 21% of the total groundwater consumption in Jiangxi province and ranking first in the province (Water Resources Department of Jiangxi Province, 2018). As one of the important sources of water supply in Ganzhou, groundwater accounted for 9%~12% of whole water supply in Ganzhou (Zeng et al., 2015). To study the relevance between groundwater extraction and the surface subsidence in the study area, this paper analysed the surrounding conditions of the study points in detail. P4 was a point surrounded by industrial parks and factories which next to an area with frequent industrial activities in the Shahe town, and there were several residential villages in the east of P4, as shown in Figure 10, the above conditions have aggravated the groundwater extraction in Shahe town. As a result, the superposition of multiple factors led to extremely serious surface subsidence in the P4 area, with the maximum cumulative surface subsidence reached 50.2mm, as shown in Figure 11, it was also the most heavy surface subsidence area in

the study area. As shown in Figure 12, the overall cumulative surface subsidence of the P1 and P2 areas was significantly larger than the other study points. It can be learned that the P1 and P2 areas were residential areas by observing the surrounding conditions. The impact of human engineering activities mentioned in the previous article has led to the deformation situation of P1 and P2 is more serious than sparse residential area. Therefore, the groundwater extraction has a great correlation with the surface deformation.



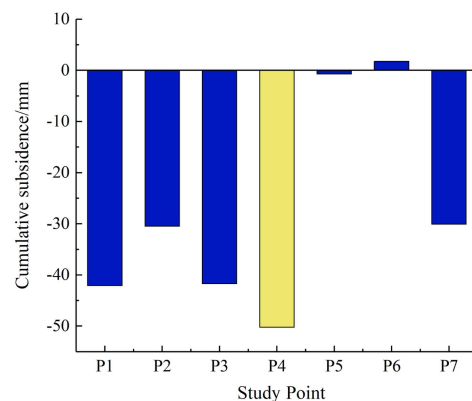**Figure 10.** Surface subsidence rate around P4 and surrounding satellite image



**Figure 11.** The final cumulative surface subsidence of each study point
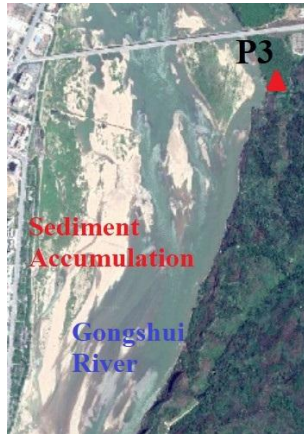


**Figure 12.** Surface subsidence rate around P1 and P2 and surrounding satellite image

## 5.6 River sediment accumulation

The Ganjiang River Section, Zhangjiang River Section, and Gongshui River Section in the planned area of Ganzhou City are all located within the confines of the reservoir. Affected by the backwaters, the sediment accumulation of the river channels in these sections will be intensified. As shown in Figure 13, it can be seen that the P3 point area is the most serious part of the river sedimentation in the study area. Due to the high

compression ratio of silty soil, the foundation soil with silty soil layer is very easy to produce compression deformation, which leads to uneven subsidence of the foundation (Liu, 1994; Panggea et al., 2021). At the same time, the maximum cumulative surface subsidence of the P3 area reached 41.7mm. In summary, it can be concluded that the river sediment accumulation had an impact on the surface subsidence of the study area.



**Figure 13.** Satellite imagery and surface subsidence rate around P3

## 6. CONCLUSION

In this paper, surface subsidence in Ganzhou area was firstly derived by SBAS-InSAR technology based on 24 Sentinel-1A SAR images. Then the temporal and spatial characteristics of the land subsidence in the study area from September 2018 to August 2020 were obtained. Finally, the main reasons for the subsidence were analysed in detail. The main conclusions are as following:

1. During the study period, the surface subsidence was uneven in this area, but the surface subsidence in most areas was relatively small, and the average surface subsidence rate was maintained from 3 to 5.4 mm/a. The areas with severe surface subsidence were mainly distributed in Ganxian District; in addition, the data internal coincidence accuracy evaluation showed that the detection accuracy was high, and most of the average rate standard deviation was concentrated in 2 mm/a, which indicated that the results were good.

2. The most serious surface subsidence area was the area of Shahe Town, where the P4 was located, and the cumulative surface subsidence has reached 50mm. The remaining areas with serious surface subsidence were the Xinlidongyuan neiborhood area in Meilin Town, the intersection of Gaoxin highway and Chengbei highway in Meilin Town, the Gongshui River section, and the Fuyutang Village of Shahe Town.

3. The comparative analysis of surface subsidence and influencing factors in this area showed that precipitation, human engineering activities, groundwater extraction, and river sediment accumulation are the main factors that cause uneven surface subsidence in the study area.

## ACKNOWLEDGEMENTS

## REFERENCES

Wu, Q., Jia, C.T., Chen, S.B., Li, H.Q., 2019. SBAS-InSAR Based Deformation Detection of Urban Land, Created from Mega-Scale Mountain Excavating and Valley Filling in the Loess Plateau: The Case Study of Yan'an City. *Remote Sensing*, 11(14), 1673-1693.

Chen, Y., Tong, Y.X., Tan, K., 2020. Coal Mining Deformation Monitoring Using SBAS-InSAR and Offset Tracking: A Case Study of Yu County, China. *IEEE Journal of Selected Topics in Applied Earth Observations and Remote Sensing*, 13, 6077-6087.

Singleton, A., Li, Z., Hoey, T., Muller J.-P., 2014. Evaluating sub-pixel offset techniques as an alternative to D-InSAR for monitoring episodic landslide movements in vegetated terrain. *Remote Sensing of Environment*, 147, 133-144.

Sánchez-Gámez, P., Navarro, F.J., 2017. Glacier Surface Velocity Retrieval Using D-InSAR and Offset Tracking Techniques Applied to Ascending and Descending Passes of Sentinel-1 Data for Southern Ellesmere Ice Caps, Canadian Arctic. *Remote Sensing*, 9, 442-459.

Hu, J., Li, Z.W., Ding, X.L., Zhu, J.J., Zhang, L., Sun, Q., 2012. 3D coseismic Displacement of 2010 Darfield, New Zealand earthquake estimated from multi-aperture InSAR and D-InSAR measurements. *Journal of Geodesy*, 86, 1029-1041.

Berardino, P., Fornaro, G., Lanari, R., Sansosti, E., 2002. A new algorithm for surface deformation monitoring based on small baseline differential SAR interferograms. *IEEE Transactions on Geoscience and Remote Sensing*, 40(11), 2375-2383.

Bateson, L., Cigna, F., Boon, David., Sowter, Andrew., 2015. The application of the Intermittent SBAS (ISBAS) InSAR method to the South Wales Coalfield, UK. *International Journal of Applied Earth Observation and Geoinformation*, 34, 249-257.

Zhou, L., Guo, J.M., Hu, J.Y., Li, J.W., Xu, Y.F., Pan, Y.J., Shi, M., 2017. Wuhan Surface Subsidence Analysis in 2015–2016 Based on Sentinel-1A Data by SBAS-InSAR. *Remote Sensing*, 9(10), 982-1002.

Ali, M., 2021. Monitoring the Iran Pol-e-Dokhtar flood extent and detecting its induced ground displacement using sentinel 1 imagery techniques. *Natural Hazards*, 105, 2603-2617.

Mo, Y., Jiang, L.M., Sun Q.S., Zhu, Y.F., 2020. Monitoring and analysis of land subsidence in Shangyu area of Hangzhou Bay by SBAS-InSAR[J]. Science of Surveying and Mapping, 45(10), 77-84.

Hooper, A., Segall, P., Zebker, H., 2007. Persistent scatterer interferometric synthetic aperture radar for crustal deformation analysis, with application to Volcán Alcedo, Galápagos. *Journal of Geophysical Research-Solid Earth*, 112(B7), 1-21.

Hong, H., Naghibi, S.A., Pourghasemi, H.R., Pradhan, B., 2016. GIS-based landslide spatial modeling in Ganzhou City, China. *Arabian Journal of Geosciences*, 9, 112-138.

Liu, Y.L., Lin, S.T, Song, D.F., Chen, C., Lu, L., Qiu, Z.X., 2020. Monitoring and early warning of Monochamus alternatus

in Zhanggong district based on GIS and geostatistics. *China Plant Protection*, 40(01), 40-47.

Peng, K., Peng, H.X., Liang, F., Huang, C.S., Ma, S.H., Qiu, Z.M., 2017. Distribution Characteristics and Development Environment of Geological Disasters in Ganzhou City. *Safety and Environmental Engineering*, 24(01), 33-39.

Lv, C., Ling, M., Wu, Z., Cao, Q.Q., 2020. Quantitative assessment of ecological compensation for groundwater overexploitation based on emergy theory. *Environ Geochem Health*, 42, 733-744.

Water Resources Department of Jiangxi Province, 2018. *Jiangxi Water Resources Bulletin.*

Zeng, J.F., Li, Z.B., Zhong, J., 2015. Analysis and Research Conception of Urban Hydrological Effect in Ganzhou City. *Pearl River*, 36(01), 50-53.

Liu, L.H., 1994. Environmental geological problems in the development and utilization of water and soil resources in the planning district of Ganzhou City, Jiangxi Province. *Jiangxi Geology*, 3, 219-224.

Panggea, G., Asep, S., Koki, K., Katsuaki, K., 2021. Combined SBAS-InSAR and geostatistics to detect topographic change and fluid paths in geothermal areas. *Journal of Volcanology and Geothermal Research*, 416, 107272-107289.